Nuclear Physics

Lucas Thoennes

Published 3-29-2018

Department of Physics and Astronomy, University of New Mexico
1 University of New Mexico, Albuquerque, NM 87131
lthoennes@unm.edu

ABSTRACT: Two thallium-activated sodium iodide (NaI(Tl)) scintillation detector based experiments were conducted. One with intent of showing decay schemes of various radioactive sources, empirically discover the attenuation coefficients of gamma rays as a function of energy and determine the identity of an unknown isotope from a laboratory obtained isotope library. The second experiment investigates the muon's mean lifetime using statistics from cosmic ray generated muons slowed in a large barrel size scintillator. The muon will be shown to have a decay lifetime of 1.91±0.14 μs.

INTRODUCTION: Scintillation detection is used in both of the following experiments. Even though the volume of the NaI(Tl) is very different between the two experiments the measurement concept is very similar. A photomultiplier tube (PMT) will be used in both experiments as well. Figure 1 below shows an idealized NaI(Tl) scintillator with PMT attached. As it relates to experiment 1, it is important to note this apparatus was placed inside a ~.5 m^3 cave made of lead bricks, with the gamma radiation source placed a few centimeters away from the NaI crystal. For experiment 2 the NaI(Tl) is a considerable volume of barrel proportions, so the PMTs used are in some way submersed into a mineral bath [1] to allow scintillation detection.

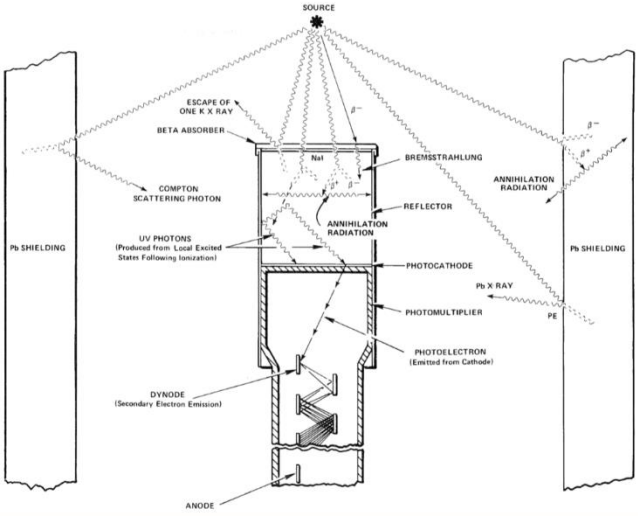

Figure 1: Idealized NaI based scintillation detector.

The gamma ray sources for each experiment couldn't be more different. For experiment 1, coin sized chips of known purified radioactive samples are provided. These include Cs^{137}, Co^{60}, Co^{57}, Na^{22}, Mn^{54}, Ba^{133} and Cd^{109}. For experiment 2 the scintillation medium and cosmic radiation provide our gamma sources. Cosmic rays interact with particles in our atmosphere to create muons [2], which are traveling at a very high velocity. The goal is to measure those muons which have just enough kinetic energy to be stopped by the scintillation medium in the lab and then experience a decay while inside the scintillation crystal. Both of the experiments share the fundamental mechanism that what is actually being measured is the gamma ray emitted from an individual NaI molecule as it rearranges its electron shell. [3] This gamma ray is measured as a current pulse in the PMT, which is detectable due to the high voltage sources in both experimental setups. This deexcitation of the electron shell configuration in the sodium iodide is one of the key reasons for its longstanding use as a scintillation medium, since it provides a near linear response across a broad range of incident gamma energies but also the speed at which the gamma emission occurs (~250ns) is very fast compared to other medium. [4] The reported resolution of a common NaI based detector is 7-9 % for incident gamma energies of 662 KeV. [5]

EXPERIMENT 1: A schematic for the design of this experiment is shown in Figure 2. Using this, in conjunction with Figure 1 earlier a basic idea for the experimental concept can be explained. The scintillation crystal (NaI(Tl)), photomultiplier tube (PMT), and base are all one unit. The radioactive source is placed ~ 4 cm away from the detector inside a lead shielded cave. As the source experiences energetic decay's these will interact with the scintillation crystal and cause gamma ray emission. These gamma rays are then converted into photoelectrons at the PMT, multiplied by the ~1200 V high voltage power supply (HV), and measured as a current pulse after amplification.

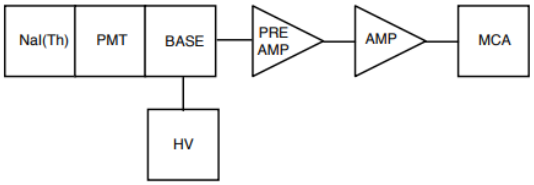

Figure 2: Schematic of experiment 1.

It is important to note that the current pulses detected by the multichannel analyzer (MCA) will not all be proportional to energies of known isotope decays being referenced here. [6] There will be many gamma rays incident on the scintillator including those that first interact with the lead cave walls causing them to change frequency [7], those that have interacted with *other* gamma rays, as well as unavoidable environmental noise including the emission of gamma rays from the nearby concrete wall materials since the lead brick cave is not 'light tight'. There is also an angular dependence when considering the cross section of Compton scattering which can create not only a photoelectron that causes a pulse detection but also creates a less energetic gamma ray that will interact with the crystal again. For the range of energies in this experiment the dominant gamma ray to matter interaction cross section is Compton Scattering, which produces an energetic electron(s) as well as having a remainder gamma ray the is less energetic than the original gamma ray incident on the scintillator. The photon cross section most directly related to the total conversion of the gamma ray to visible light is the photoelectric effect.

Figure 3 shows a spectrum of current pulses detected by the PMT against the number of those pulses detected for a sample of Cs^{137}.

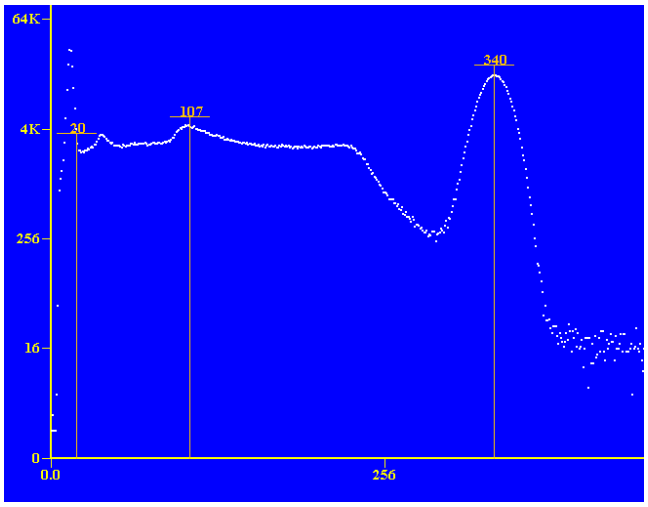

Figure 3: Cs 137 spectrum

The spectrum in Figure 3 shows a distinct peak at channel number 340 with counts in the thousands over the ten minute sampling period. This photopeak is directly proportional to the decay energy of the transition from Cs^{137} to Ba^{137}. [8] Each of the radioactive samples provided in lab will have one or more of these characteristic photopeak's. An example is Co^{60} shown in Figure 4 below. This isotope of Cobalt has two gamma emissions during its decay to Ni^{60}, corresponding to photopeaks at channel 591 and 668.

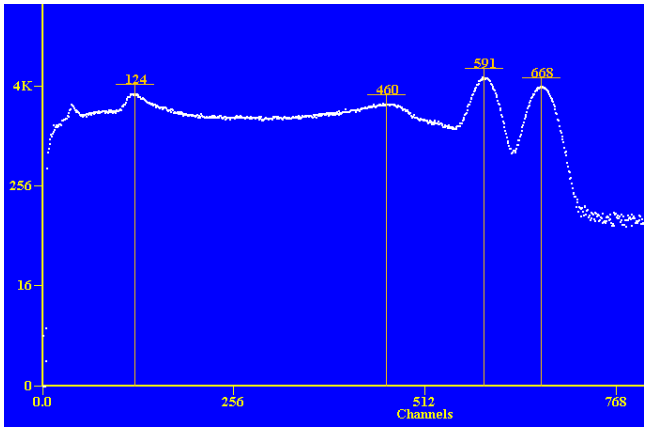

Figure 4: Co-60 spectrum

Using the knowledge of the photopeak energies for each sample along with spectrum graphs for each, Table 1 below can be constructed.

Photopeak	Energy (MeV)	Channel #
Cs^{137}	0.662	340
Co^{60}	1.17	591
Co^{60}	1.33	668
Co^{57}	0.122	66

Table 1: Calibration values

Calibration using the values in Table 1 allows a relation between the bin the electrical pulse of a certain magnitude is placed and the energy of the scintillation. A plot of these values as in Figure 5 shows the linearity of energy with channel number, a byproduct of choosing thallium-activated sodium iodide.

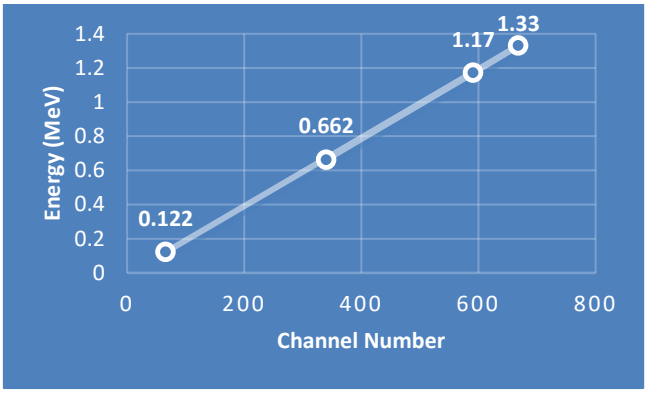

Figure 5: Energy Calibration Curve for NaI(Tl) detector

This calibration provides a mechanism to carry out some simple sample identification using this setup. The mystery sample provided to us has a spectrum as shown in Figure 6 below.

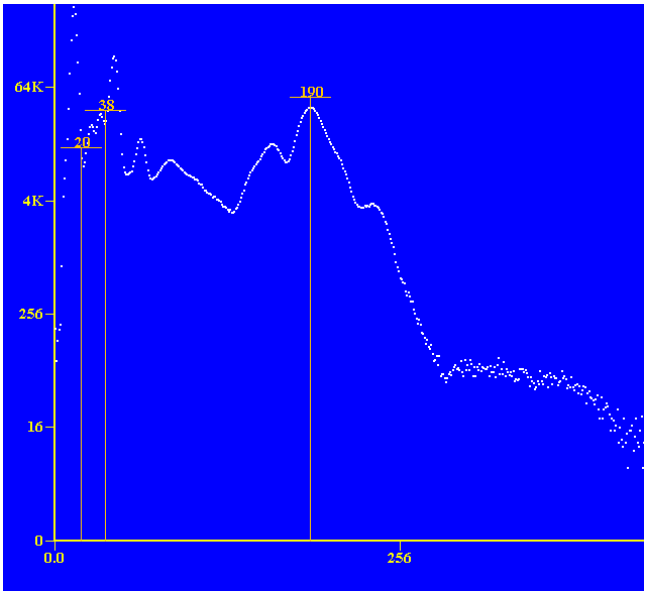

Figure 6: Unknown sample's spectrum

The calibration curve obtained in plotting Figure 5 gives a simple formula for the energy given a channel.

$$E = 0.002 * C - 0.0139 \quad (1)$$

Where E is the energy in MeV, and C is the channel number the MCA sorted the current pulse into. For the unknown sample a distinct peak at 190 is seen. This would correspond to an energy measurement of 366±7 MeV. Ba^{133} is known to experience a gamma emission of magnitude 366 MeV [9]. An isotope library that included each gamma source available in the lab was gathered. This allowed the comparison between the unknown sample spectrum and the libraries version of Ba^{133} which proved to be very similar. Thus, it is concluded the unknown sample was Barium 133.

Finally, a determination of the gamma ray attenuation coefficients. Equation 2 gives a simple relation between the number of transmitted source photons sent towards the detector and the number that reach the detector after passing through the matter between. [10]

$$I = I_0 e^{-\mu t} \quad (2)$$

The total counts of monoenergetic photons I_0 can be obtained by collecting data with nothing blocking the source. Then thin discs of lead and copper can be placed directly between the detector and the source, at varying thicknesses. Table 2 contains this data.

Metal	Thickness (mm)	Energy (MeV)	Counts
	0	0.662	4791
	0	1.17 , 1.33	5326, 4290
Lead	5	0.662	2659
Lead	10	0.662	1436
Lead	15	0.662	811
Lead	5	1.17 , 1.33	2999, 2396
Lead	10	1.17 , 1.33	1911, 1484
Lead	15	1.17 , 1.33	1089, 884
Copper	10	0.662	2225
Copper	15	0.662	1971
Copper	25	0.662	1032
Copper	10	1.17 , 1.33	2125, 1792

Copper	15	1.17 , 1.33	1501, 1172
Copper	25	1.17 , 1.33	714, 520

Table 2: Attenuation coefficient data.

Each sampling in Table 2 was for 600 seconds. Using this constraint and Equation 2, a plot of transmitted photons verses absorber thickness is obtained as in Figure 7a and 7b.

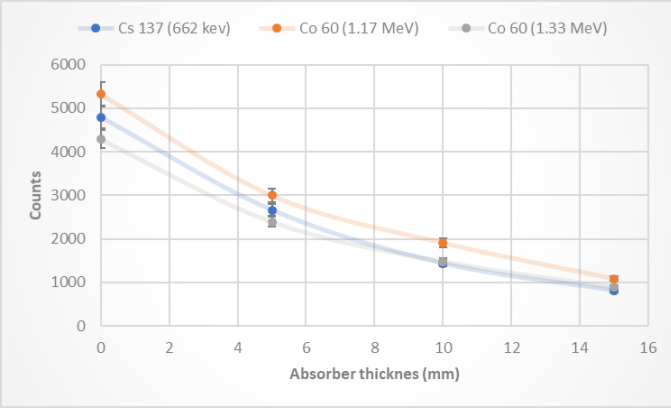

Figure 7a: Change in measured gamma ray counts with varied thickness of lead absorber between the source and detector.

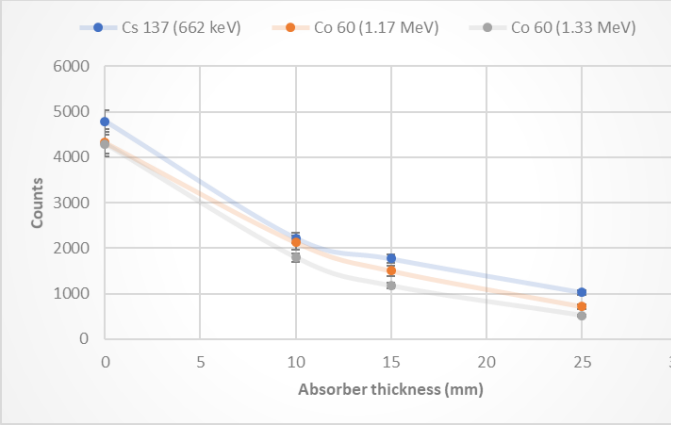

Figure 7b: Change in measured gamma ray counts with varied thickness of copper absorber between the source and detector.

The plots above both indicate a nonlinear, exponential relation between attenuation of the gamma rays as they pass through the absorber medium at these distances. The increasing length of the error bars in the figures as absorber thickness approaches zero is due to the statistical uncertainty in counting statistics given as

$$\delta N = \sqrt{N} \qquad (3)$$

Where N is the noise stripped counts output by the MCA. Equation 2 can be solved for the two different absorber materials used, lead and copper, to arrive at the following table. By inspection a dependence on energy of the gamma ray incident on the material can be concluded. Comparing the values obtained in Table 3 with the accepted values for μ for lead at an energy of 662 MeV we measured 0.119 cm^2/gram (using a density of 11.34 gram/cm^3) which is above the accepted value of 0.105 cm^2/gram. Our value for copper was also higher than the accepted value, arriving at a value of 0.068 cm^2/gram (using a value of 8.96 gram/cm^3).

Absorber - E_γ	Thickness (mm)	Attenuation Coefficient μ (mm^{-1})
Lead – 662 keV	5	117.75±5.88
Lead – 662 keV	10	120.48±6.02
Lead – 662 keV	15	118.41±5.94
Lead – 1.17 MeV	5	114.86±5.54
Lead -1.17 MeV	10	102.49±5.1
Lead – 1.17 MeV	15	105.82±5.19
Lead – 1.33 MeV	5	116.49±5.77
Lead – 1.33 MeV	10	106.15±5.75
Lead – 1.33 MeV	15	105.3±5.19
Copper – 662 keV	10	76.69±3.83
Copper – 662 keV	15	59.21±2.96
Copper – 662 keV	25	61.4±3.01
Copper – 1.17 MeV	10	91.88±4.5
Copper – 1.17 MeV	15	84.43±4.12
Copper – 1.17 MeV	25	80.37±4.08
Copper – 1.33 MeV	10	87.29±4.25
Copper – 1.33 MeV	15	86.5±4.18
Copper – 1.33 MeV	25	84.4±4.08

Table 3: Calculated attenuation coefficients.

EXPERIMENT 2: This experiment investigates the decay of muons. Figure 8 shows a schematic of the experimental setup. Depicted are two muons, one passing through the NaI(Tl) scintillation detector the other ranging out inside the detector medium and experiencing a decay which produces an electron. Instead of just a single PMT like in experiment 1, two are used each connected to an MCA and dedicated counting circuit board, which is then fed into a PC running LabVIEW.

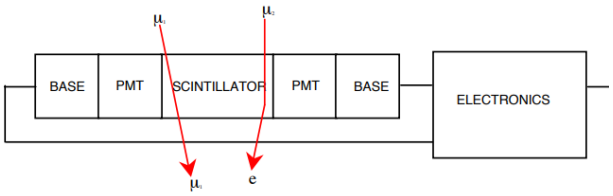

Figure 8: Muon decay experimental setup.

Measurement in this experiment will focus on muons that have come to a complete stop in the scintillation crystal and then experienced a decay emitting an electron. This will produce a pair of pulses that can be counted, whereas a muon that passes through the detector without stopping and emitting an electron will produce only one pulse. Much like experiment 1, an MCA will group the detected gamma emissions into bins proportional to the energy of the gamma ray detected. However, this experiment has additional setup due to the use of two detectors. Utilizing both detectors allows for a coincident triggering. This means that a timeframe between the detection of scintillation energy needs to be set, which has a benefit of reducing counts due to noise. Our coincident timing was set at 40 ns, which means that the detectors will both need to register a scintillation above a certain energy threshold with 40 ns of each other in order for the count to be registered. There is also a need for a gate width time, which is a threshold that LabVIEW uses to decide when a decay detection is from one scintillation or an overlap of two separate detections that occurred very close to each other. We found that a gate width time of 10 ms (about 5 muon lifetimes) gave the clearest data, as shown in Figure 9.

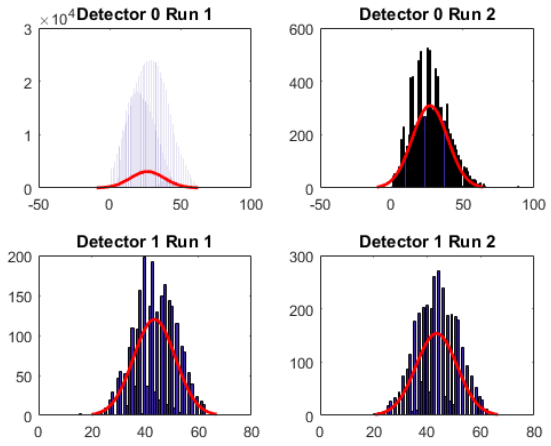

Figure 9: Detection counts for varied time scales.

As expected, a Gaussian shape emerges in the plots with the mean (central peak position for an ideal Gaussian) being proportional to the average energy of the detected muons. The fact that different run times are used for the four plots in Figure 9, ranging from a few minutes to a whole week, yet a Gaussian shape centered at a similar value (ignoring detector performance differences) is shown indicates that the distribution of muon energies is similar regardless of run time and only the number of muons reaching the detector changes, not the average energy of the slowed muon.

Using a similar approach to the muon energy measurements, an approximation of the muon lifetime can be made. Figure 10 shows a semi-log plot of the data captured for muon decay. A linear fit (red line) to this data set allows us to solve for the muon decay lifetime to first order using Equation 3 below.

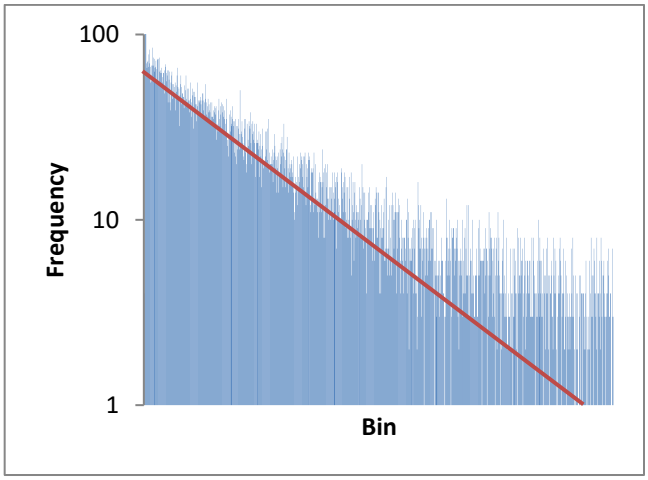

Figure 10: Histogram of muon decay scintillation captures.

$$N(t) = N_{stop} e^{-\frac{t}{\tau_\mu}} \qquad (3)$$

The inverse negative of the red linear fit line gives a value for the muon decay time of 1.91±0.14 μs. This is slightly below the actual accepted value of 2.2 μs.

Summary: These two experiments have revealed atomic level interactions that are actually occurring constantly in nature. Bombardment of particles in our atmosphere create energetic particles travelling at relativistic speeds, that can be detected here on the ground. Spontaneous decays of elemental matter emit gamma rays of a constant energy which can be used to identify

what the source is. One further concept is worth mentioning that relates to the detection equipment used. A basic, yet complicated, question is that for a given PMT (and high voltage source) what is the relationship between the energy of the gamma ray incident on the scintillation crystal and the number of photoelectrons created by this interaction? Obviously, this can only be a rough approximation, as the actual multiplicity of the generated electrons is a complicated property but to first order an interesting approximation can be made. To first approximation the full width half max (FWHM) of a known photopeak has a simple relation with the resolution of the detector given by Equation 4. [11]

$$\frac{FWHM}{2.35} = \frac{E_\gamma}{\sqrt{N_e}} \quad (4)$$

Where E_γ is the energy of the emitted photon and N_e is the number of photoelectrons before amplification. Using our Cs^{137} source as our reference we find a FWHM of 28 for the 662 keV energy. Using Equation 4 we find a value for the number of created photoelectrons of $3x10^9$! This rough approximation shows just a single gamma ray with an energy of around half an MeV can produce billions of photoelectrons when interacting with this type of scintillation medium. No wonder a current can be measured!

REFERENCES:

[1] W.R. Leo, Ch. 7, Scintillation Detectors.
[2] F. Halzen and A.D. Martin, Quarks and Leptons: an Introductory Course in Modern Particle Physics, (Wiley, New York, 1984).
[3] G.F. Knoll, Radiation Detection and Measurement, Ch. 7, 2nd Ed. (Wiley, New York, 1989).
[4] G.F. Knoll, Radiation Detection and Measurement, Ch. 5, 2nd Ed. (Wiley, New York, 1989).
[5] Harshaw Radiation Detectors, Harshaw/Filtrol, 6801 Cochran Rd., Solon, Ohio report FWHM/Eγ ~ 7-9 % at 662 KeV for NaI(Tl) detectors.
[6] C.M. Lederer and V.S. Shirley, Table of Isotopes, 7th Ed. (Wiley, New York, 1978).
[7] W.R. Leo, Ch. 8, PMTs.
[8] W.R. Leo, Ch. 14, Pulse Signal Shaping and MCAs.
[9] Wikipedia contributors. "Isotopes of barium." Wikipedia, The Free Encyclopedia. Wikipedia, The Free Encyclopedia, 6 Mar. 2018. Web. 17 Mar. 2018.
[10] G.F. Knoll, Radiation Detection and Measure ment, Ch. 2, 2nd Ed. (Wiley, New York, 1989).
[11] Lab Manual